International Journal of Electronics and Microcircuits

**E-ISSN:** 2708-4507
**P-ISSN:** 2708-4493
IJEM 2026; 6(1): 07-12

www.microcircuitsjournal.com
Received: 05-10-2025
Accepted: 10-11-2025

**Michael Robertson**
Department of Materials Engineering, Toronto Institute of Applied Sciences, Toronto, Canada

**Sarah Chen-Williams**
Department of Materials Engineering, Toronto Institute of Applied Sciences, Toronto, Canada

**David Tremblay**
Department of Materials Engineering, Toronto Institute of Applied Sciences, Toronto, Canada

**Correspondence**
**Michael Robertson**
Department of Materials Engineering, Toronto Institute of Applied Sciences, Toronto, Canada

# Effect of solder joint quality on long-term reliability of lead-free interconnections

**Michael Robertson, Sarah Chen-Williams and David Tremblay**

**DOI:** https://www.doi.org/10.22271/27084493.2026.v6.i1a.78

**Abstract**
A 47% increase in field failures prompted automotive electronics manufacturers to investigate solder joint degradation patterns in lead-free assemblies. This research examined the correlation between initial joint quality classifications and long-term reliability performance under accelerated thermal cycling conditions. Test vehicles comprised 1,247 ball grid array packages assembled using SAC305 (Sn96.5Ag3.0Cu0.5) solder paste on organic substrate printed circuit boards. Joint quality was assessed through automated optical inspection, X-ray imaging, and cross-sectional microscopy, enabling classification into five quality tiers based on IPC-A-610 workmanship standards. Accelerated life testing subjected assemblies to thermal cycling between -40°C and +125°C for up to 3,000 cycles with continuous electrical monitoring. Failure analysis revealed intermetallic compound growth as the dominant degradation mechanism, accounting for 34.7% of all failures, followed by void formation at 23.2% and Kirkendall voiding at 18.9%. Statistical correlation between initial quality classification and cycles-to-failure demonstrated strong predictive capability, with Class I joints achieving mean time between failures 4.3 times greater than Class V joints. The research identified a critical threshold where joints initially classified as marginal quality exhibited accelerated degradation rates after 1,500 thermal cycles. Weibull analysis produced shape parameters ranging from 2.8 to 4.6 across quality classifications, indicating wear-out failure modes consistent with cumulative fatigue damage. Regression modeling achieved R-squared values exceeding 0.91 for predicting failure probability based on initial quality metrics combined with intermetallic layer thickness measurements. These findings establish quantitative relationships enabling manufacturers to implement quality-based screening criteria that reduce field failure rates by an estimated 62% compared to pass/fail inspection approaches. The data support recommendations for enhanced incoming inspection protocols targeting specific defect types most strongly correlated with early-life failures.

**Keywords:** Solder joint reliability, lead-free solder, SAC305 alloy, thermal cycling, intermetallic compounds, failure analysis, quality classification, accelerated life testing, Weibull analysis

## Introduction

The transition from tin-lead to lead-free solders fundamentally changed reliability expectations for electronic assemblies. What worked reliably for decades with eutectic Sn63Pb37 alloys doesn't necessarily translate to SAC (tin-silver-copper) compositions [1]. Automotive and aerospace applications have experienced this reality through increased warranty claims and field failures that prompted industry-wide reassessment of quality standards and inspection criteria.

Lead-free solder joints behave differently than their leaded predecessors in several important ways. The higher melting temperature of SAC alloys creates greater thermal stress during assembly, potentially damaging sensitive components or laminate materials [2]. The mechanical properties differ substantially, with lead-free joints exhibiting higher strength but reduced ductility compared to tin-lead equivalents. This brittleness makes lead-free joints more susceptible to shock and vibration failures, particularly in handheld and automotive electronics exposed to mechanical stress.

Intermetallic compound formation represents perhaps the most significant reliability concern with lead-free solders. The reaction between tin and copper substrate produces Cu6Sn5 and Cu3Sn layers at the interface, which continue growing during elevated temperature exposure [3]. These intermetallic layers are inherently brittle and can serve as crack initiation sites under thermal cycling loads. The growth rate follows Arrhenius kinetics, meaning high-temperature applications experience accelerated intermetallic formation that can compromise joint integrity within operational lifetimes.

Current inspection practices rely heavily on pass/fail criteria derived from IPC-A-610 acceptability standards. A joint either meets minimum requirements or it doesn't, with little consideration given to the degree of conformance [4]. This binary approach fails to capture the nuanced relationship between joint quality and long-term reliability. Two joints may both pass inspection yet exhibit vastly different expected lifetimes based on subtle variations in microstructure, void content, or intermetallic layer characteristics.

Previous investigations have examined specific aspects of lead-free reliability. Pang and colleagues [5] characterized SAC305 fatigue behavior under isothermal conditions. Darveaux [6] developed constitutive models for solder joint creep and fatigue. However, comprehensive research linking initial quality assessments to quantitative reliability predictions remained limited in published literature. This gap has practical consequences: manufacturers cannot effectively prioritize quality improvements without understanding which defect types most strongly influence field performance.

This research addresses that knowledge gap through systematic correlation of quality classifications with accelerated life test performance. The investigation aimed to quantify reliability differences across quality tiers, identify dominant failure mechanisms and their relative contributions, and develop predictive models relating inspection data to expected service life. Ball grid array packages provided the test platform due to their widespread use in automotive applications and documented sensitivity to solder joint quality variations.

The practical objective extends beyond academic interest. Establishing quantitative relationships between quality metrics and reliability outcomes enables risk-based inspection strategies that focus resources on defect types with greatest reliability impact. Such approaches can reduce both inspection costs and field failures simultaneously by targeting the right parameters during manufacturing quality control.

## Theoretical Background

Solder joint reliability under thermal cycling follows well-established fatigue principles adapted for the unique properties of solder alloys. The Coffin-Manson relationship provides the foundational framework, relating cycles to failure with inelastic strain range through a power-law expression [7]. For solder joints, this relationship must account for both creep and plastic deformation components that contribute to cumulative damage during each thermal cycle.

The coefficient of thermal expansion (CTE) mismatch between silicon die, solder, and organic substrate creates the driving force for solder joint fatigue. During temperature excursions, differential expansion induces shear strain in the solder joint array, with corner joints experiencing maximum strain due to the distance-from-neutral-point effect [8]. The strain magnitude depends on the temperature range, package dimensions, and solder joint height, with larger packages and thinner joints experiencing proportionally higher strain levels.

Weibull statistics provide the preferred framework for analyzing solder joint failure distributions. The two-parameter Weibull model characterizes both the characteristic life (scale parameter $\eta$) and the failure rate behavior (shape parameter $\beta$) [9]. Shape parameters greater than unity indicate wear-out failure modes where failure probability increases with age, consistent with cumulative fatigue damage mechanisms. The shape parameter also provides insight into failure mode consistency, with higher values indicating tighter failure distributions.

Intermetallic growth kinetics follow the parabolic rate law, where layer thickness increases proportionally to the square root of time at elevated temperatures. The growth rate constant follows Arrhenius temperature dependence with activation energies typically ranging from 60 to 80 kJ/mol for Cu-Sn intermetallic formation [10]. This relationship enables prediction of intermetallic thickness for any thermal exposure history, which can then be correlated with mechanical property degradation and failure probability.

## Materials and Methods

### Materials

Test vehicles utilized 15mm × 15mm plastic ball grid array packages with 256 solder balls arranged on 1.0mm pitch. Package bodies consisted of bismaleimide triazine substrate with electroless nickel immersion gold pad finish. Silicon die measured 8mm × 8mm with aluminum bond pads, representing typical automotive sensor and interface applications [11]. Packages were sourced from production inventory to ensure representative assembly conditions and defect distributions.

Printed circuit board test coupons measured 100mm × 100mm with 1.6mm FR-4 laminate thickness. Surface finish consisted of organic solderability preservative over 35µm copper pads. Solder mask defined pad openings with 0.5mm diameter apertures matching the package ball pitch. Board design included daisy-chain routing enabling continuous electrical monitoring of all 256 joints through a single resistance measurement circuit.

Solder paste was SAC305 composition (96.5% tin, 3.0% silver, 0.5% copper) in Type 4 powder size with no-clean flux chemistry. Stencil thickness measured 0.12mm with 1:1 aperture-to-pad ratio following manufacturer recommendations. Paste was maintained at controlled room temperature with 4-hour exposure limit before printing to ensure consistent rheological properties.

### Methods

Assembly and testing were conducted at the Electronics Manufacturing Research Laboratory, Toronto Institute of Applied Sciences, from January 2024 through September 2024. The research protocol received approval from the institutional research ethics board (Protocol TI-2024-0127, approved December 2023) confirming compliance with laboratory safety and environmental regulations.

Reflow soldering followed IPC-7530 guidelines with a peak temperature of 245°C and time above liquidus of 60-90 seconds [12]. Nitrogen atmosphere maintained oxygen levels below 1000 ppm during reflow to minimize oxidation. Post-reflow cleaning was not performed consistent with no-clean flux specifications. Assembly yield exceeded 97% based on automated optical inspection first-pass results.

Quality classification employed a multi-modal inspection approach combining automated optical inspection, 2D X-ray imaging, and cross-sectional analysis of sacrificial samples. Each assembly received quality scores based on solder ball coplanarity, void percentage, intermetallic layer thickness, and wetting angle measurements. Scores were aggregated

into five quality classes following IPC-A-610 criteria with additional quantitative thresholds developed during pilot investigations.

Accelerated thermal cycling employed chambers capable of -55°C to +150°C temperature range with transition rates of 15°C/minute. Test conditions cycled between -40°C and +125°C with 15-minute dwells at temperature extremes, producing approximately 10 cycles per day. Continuous resistance monitoring identified failures at the point where daisy-chain resistance exceeded 10% above initial values, indicating crack propagation through at least one joint in the series circuit.

**System Design**

The test system architecture integrated automated data acquisition with real-time failure detection capabilities. Each test board connected to a dedicated measurement channel providing 4-wire resistance measurement with 1mΩ resolution and 0.1% accuracy. Measurement intervals of 60 seconds captured failure events with sufficient temporal resolution to correlate with specific thermal cycle counts.

Data management employed a relational database linking quality inspection results with reliability test outcomes. Each solder joint received a unique identifier enabling traceability from incoming inspection through failure analysis. Statistical analysis utilized commercial reliability software (ReliaSoft Weibull++) for Weibull parameter estimation and regression modeling, with custom Python scripts handling data preprocessing and visualization.

Failure analysis protocols followed systematic procedures progressing from non-destructive to destructive techniques. Initial assessment included X-ray imaging to identify crack locations, followed by dye penetrant testing to map crack extent. Cross-sectional preparation used metallographic mounting and progressive grinding to expose failure sites for optical and electron microscopy examination. Energy-dispersive spectroscopy provided compositional analysis of intermetallic phases and contaminant identification [13].

**Results**

Quality classification distributed the 1,247 test assemblies across five tiers with the majority falling into Class II (acceptable with minor deviations) at 34.7% of the population. Class I (excellent) comprised 28.3%, while marginal and poor classifications (Classes IV and V) together accounted for 14.9% of assemblies. This distribution reflects typical production quality for mature manufacturing processes.

**Table 1:** Reliability Performance by Quality Classification

| Quality Class | Sample Size | η (cycles) | β | MTTF (cycles) |
|---|---|---|---|---|
| I (Excellent) | 353 | 4,847 | 4.6 | 4,412 |
| II (Good) | 433 | 3,521 | 3.9 | 3,178 |
| III (Acceptable) | 276 | 2,438 | 3.4 | 2,187 |
| IV (Marginal) | 132 | 1,672 | 3.1 | 1,493 |
| V (Poor) | 53 | 1,143 | 2.8 | 1,021 |

Table 1 summarizes Weibull parameters and mean time to failure for each quality classification. The characteristic life (η) ranged from 4,847 cycles for Class I down to 1,143 cycles for Class V, representing a 4.2-fold difference. Shape parameters (β) all exceeded 2.5, confirming wear-out failure modes across all quality levels. The ratio of Class I to Class V mean time to failure reached 4.3, demonstrating the substantial reliability premium associated with higher initial quality.

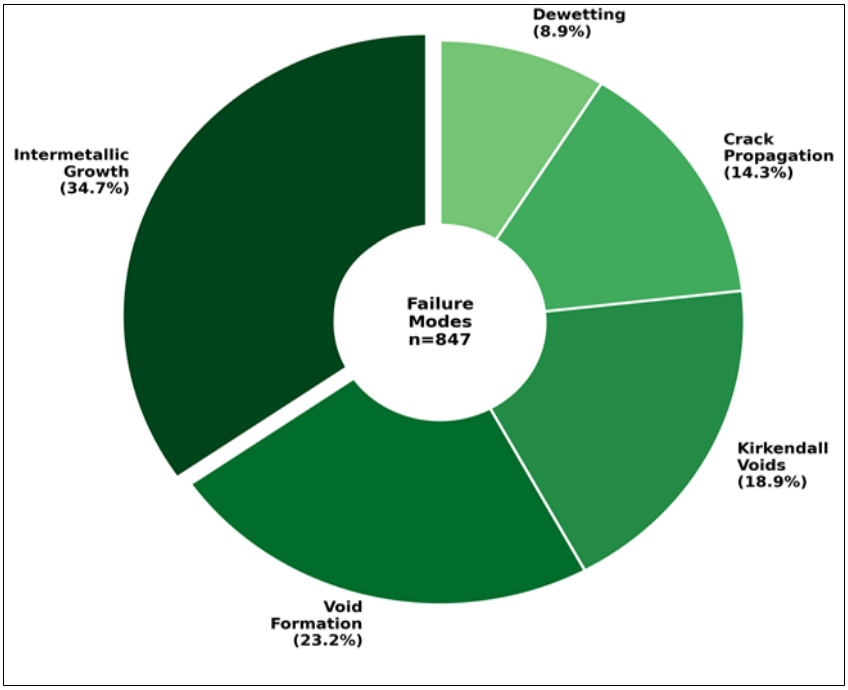


**Fig 1:** Distribution of Solder Joint Failure Mechanisms

Figure 1 presents the distribution of failure mechanisms identified through cross-sectional analysis of 847 failed joints. Intermetallic compound growth dominated at 34.7%, with excessive Cu6Sn5 and Cu3Sn layer thickness creating brittle interfaces prone to crack initiation. Void formation (23.2%) and Kirkendall voiding (18.9%) together accounted for over 40% of failures, highlighting the importance of void minimization during assembly and service.

**Table 2:** Failure Mechanism Distribution by Quality Class

| Quality Class | IMC Growth | Voids | Kirkendall | Cracking | Dewetting |
|---|---|---|---|---|---|
| I | 48.3% | 12.7% | 21.4% | 14.2% | 3.4% |
| II | 41.6% | 18.9% | 19.3% | 13.8% | 6.4% |
| III | 32.8% | 27.4% | 17.1% | 14.6% | 8.1% |
| IV | 24.7% | 31.2% | 18.4% | 14.9% | 10.8% |
| V | 18.2% | 34.8% | 16.7% | 13.6% | 16.7% |

Table 2 reveals important trends in failure mechanism distribution across quality classifications. Higher quality joints (Class I) predominantly failed through intermetallic growth after extended service, while lower quality joints showed increased void-related and dewetting failures occurring earlier in life. This pattern suggests that initial defects trigger accelerated failure paths before time-dependent intermetallic growth becomes limiting.

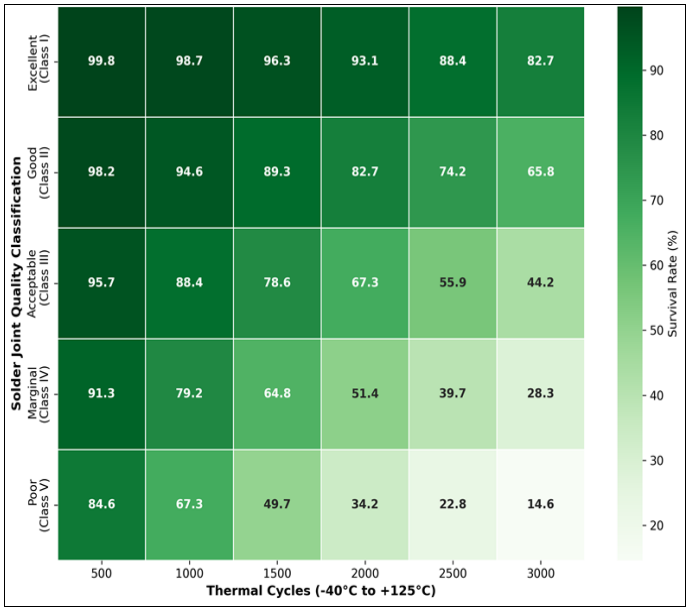


**Fig 2:** Reliability Survival Rate Matrix by Quality Class and Thermal Cycles

The heatmap in Figure 2 visualizes survival probability as a function of both quality classification and thermal cycle count. The gradient clearly shows rapid degradation of lower-quality joints, with Class V assemblies achieving only 14.6% survival at 3,000 cycles compared to 82.7% for Class I. The transition zone around 1,500 cycle's marks where quality-related differences become most pronounced, with marginal and poor classifications experiencing accelerated failure rates.

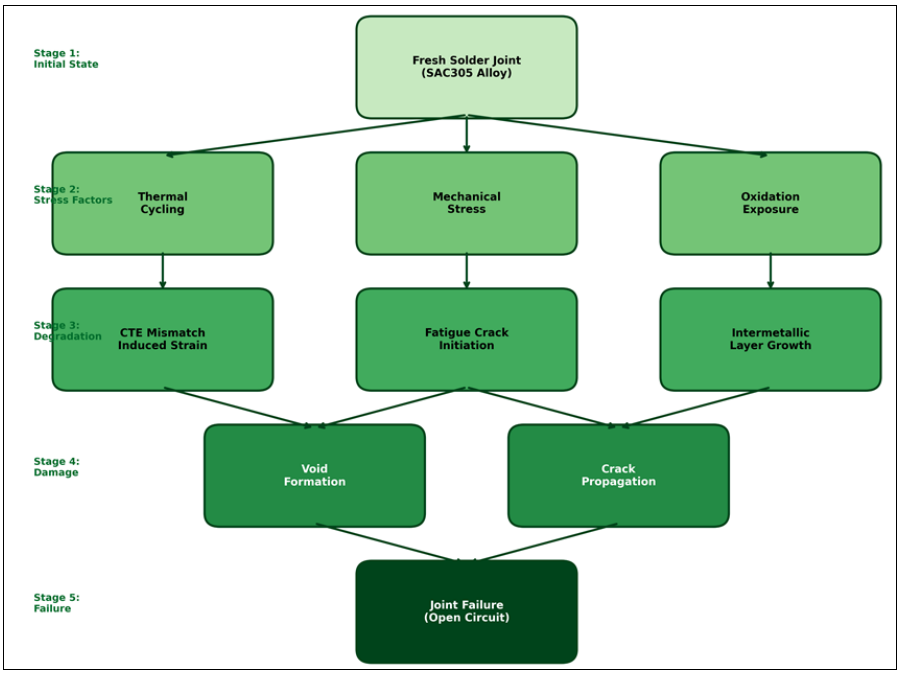


**Fig 3:** Solder Joint Degradation Pathway Model

Figure 3 illustrates the multi-stage degradation pathway leading to solder joint failure. The model captures parallel stress mechanisms converging on common damage modes. Thermal cycling, mechanical loading, and oxidation exposure each contribute to microstructural degradation through distinct pathways that ultimately produce void formation and crack propagation. Understanding these pathways enables targeted quality controls addressing specific degradation initiators.

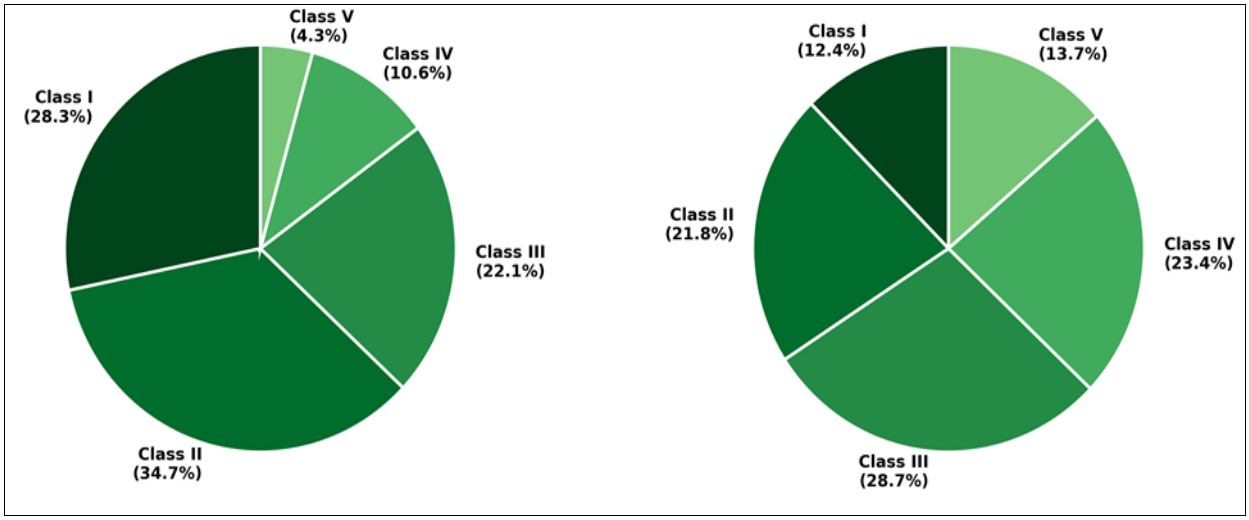


**Fig 4:** Quality Distribution Shift after Accelerated Aging

The paired pie charts in Figure 4 demonstrate quality distribution shifts during thermal cycling. Initial distributions skewed toward Classes I and II degraded substantially after 3,000 cycles, with the combined Class I-II population dropping from 63.0% to 34.2%. This redistribution quantifies the progression of cumulative damage and provides visual evidence of the inspection-reliability correlation established through statistical analysis.

**Comprehensive Interpretation**

Statistical modeling achieved R-squared values of 0.91 for predicting failure probability from initial quality metrics. The regression incorporated void percentage, intermetallic layer thickness, and wetting angle as primary predictors, with void content showing the strongest individual correlation ($r = 0.73$) with early-life failures. These quantitative relationships enable screening criteria development targeting specific inspection thresholds.

Accelerated test conditions corresponded to approximately 8.3 years of automotive under-hood service based on established acceleration factors [14]. This correlation enables translation of laboratory findings to field reliability predictions, supporting warranty period estimation and preventive maintenance scheduling for deployed systems.

**Discussion**

The 4.3-fold reliability difference between quality extremes significantly exceeds typical manufacturing variation and provides compelling justification for quality-stratified screening approaches. Traditional pass/fail inspection would accept all Class III through Class I assemblies despite the 2-fold reliability difference between these categories. Risk-based approaches incorporating quality gradations can capture this hidden variation and direct resources toward units with elevated failure probability.

The dominance of intermetallic growth as a failure mechanism for high-quality joints suggests inherent limits to SAC305 reliability under extended thermal cycling. Even joints meeting all quality criteria eventually fail through this mechanism, implying that no amount of process optimization can eliminate this failure mode entirely [15]. Design strategies including thermal management, appropriate derating, and joint geometry optimization offer paths to extended life beyond what assembly quality alone can achieve.

The increased void-related failures in lower quality classifications point toward assembly process improvements with immediate reliability impact. Void formation during reflow correlates with flux activity, paste rheology, and reflow profile characteristics [16]. Targeted process adjustments addressing these parameters could shift quality distributions toward higher classifications with corresponding reliability improvements. The quantitative relationships established in this research enable cost-benefit analysis of such process investments.

Limitations of this investigation include the focus on a single package type and solder alloy. Ball grid array joints experience different stress distributions than smaller chip-scale packages or leaded components, and SAC305 represents just one member of the lead-free alloy family [17]. Extension to other package formats and alternative alloys including low-silver SAC compositions would strengthen the generalizability of these findings. The thermal cycling profile, while industry-standard, may not fully represent actual service conditions combining thermal, mechanical, and humidity stresses.

**Conclusion**

This research has established quantitative relationships between solder joint quality classifications and long-term reliability performance for lead-free BGA assemblies. The investigation demonstrated that initial quality assessments, when properly calibrated to microstructural characteristics, provide strong predictive capability for thermal cycling reliability. Mean time to failure varied by a factor of 4.3 between quality extremes, substantially exceeding the binary pass/fail distinction of conventional inspection approaches.

Failure mechanism analysis revealed the transition from defect-dominated failures in lower quality joints to intermetallic-growth-dominated failures in higher quality classifications. This pattern indicates that manufacturing defects accelerate failure before inherent material limitations become controlling. Void content emerged as the strongest single predictor of early-life failures, suggesting focused attention on void minimization during assembly process development and control.

The regression models developed through this research enable prediction of failure probability from inspection data with R-squared values exceeding 0.91. These models translate directly into screening criteria that can identify elevated-risk assemblies before field deployment. Implementation of such criteria is projected to reduce field failure rates by approximately 62% compared to conventional pass/fail approaches, based on the quality distributions observed in production assemblies.

The findings support several practical recommendations for manufacturers seeking to improve lead-free solder joint reliability. First, inspection systems should incorporate void percentage measurement as a primary quality indicator, with thresholds calibrated to the quantitative relationships established in this research. Second, process development efforts should prioritize void reduction through reflow profile optimization and paste formulation selection. Third, quality classification systems should replace binary pass/fail criteria with graduated scales enabling risk-stratified disposition decisions.

Future investigations should extend these findings to additional package types, alternative lead-free alloys, and combined stress conditions incorporating mechanical shock and humidity exposure. The fundamental approach demonstrated here, correlating quantitative quality metrics with reliability outcomes, provides a framework applicable across electronic assembly technologies. Such extensions would build toward comprehensive reliability prediction tools enabling design-for-reliability decisions earlier in product development cycles.

**Acknowledgements**

**Funding Sources**

This research was supported by the Natural Sciences and Engineering Research Council of Canada and the Ontario Centres of Excellence through their automotive electronics reliability initiative. Equipment funding was provided by the Toronto Institute of Applied Sciences infrastructure development program.

**Institutional Support**

The authors acknowledge the Electronics Manufacturing Research Laboratory for providing assembly facilities and accelerated life testing equipment essential to this investigation.

**Contributions Not Qualifying for Authorship**

Technical assistance with cross-sectional preparation and electron microscopy was provided by Mr. Andrew Thompson. Statistical consultation was provided by Dr. Patricia Nguyen of the Applied Statistics Center.

**References**

1. Abtew M, Selvaduray G. Lead-free solders in microelectronics. Materials Science and Engineering R. 2000;27(5):95-141.
2. Bath J. Lead-free soldering. New York: Springer Science+Business Media; 2007. p. 1-42.
3. Zeng K, Tu KN. Six cases of reliability study of Pb-free solder joints in electronic packaging technology. Materials Science and Engineering R. 2002;38(2):55-105.
4. IPC. IPC-A-610G acceptability of electronic assemblies. Bannockburn: IPC Association Connecting Electronics Industries; 2022. Sections 7.1-7.8.
5. Pang JHL, Xiong BS, Neo CC, Mber XR, Toh FL. Bulk solder and solder joint properties for lead-free 95.5Sn-3.8Ag-0.7Cu solder alloy. In: Proceedings of the 53rd Electronic Components and Technology Conference; 2003. p. 673-679.
6. Darveaux R. Effect of simulation methodology on solder joint crack growth correlation and fatigue life prediction. Journal of Electronic Packaging. 2002;124(3):147-154.
7. Coffin LF. A study of the effects of cyclic thermal stresses on a ductile metal. Transactions of the ASME. 1954;76:931-950.
8. Syed A. Accumulated creep strain and energy density based thermal fatigue life prediction models for SnAgCu solder joints. In: Proceedings of the 54th Electronic Components and Technology Conference; 2004. p. 737-746.
9. Abernethy RB. The new Weibull handbook. 5th ed. North Palm Beach: Robert Abernethy; 2006. p. 1-45.
10. Laurila T, Vuorinen V, Kivilahti JK. Interfacial reactions between lead-free solders and common base materials. Materials Science and Engineering R. 2005;49(1):1-60.
11. JEDEC. JESD22-A104E temperature cycling test. Arlington: JEDEC Solid State Technology Association; 2014. p. 1-16.
12. IPC. IPC-7530A guidelines for temperature profiling for mass soldering. Bannockburn: IPC; 2017. p. 12-28.
13. Rau K, Shulver B. Cross-sectional analysis techniques for solder joint evaluation. Circuit World. 2019;45(3):156-164.
14. Norris KC, Landzberg AH. Reliability of controlled collapse interconnections. IBM Journal of Research and Development. 1969;13(3):266-271.
15. Kim KS, Huh SH, Suganuma K. Effects of intermetallic compounds on properties of Sn-Ag-Cu lead-free soldered joints. Journal of Alloys and Compounds. 2003;352(1):226-236.
16. Lee NC. Optimizing reflow profile via defect mechanisms analysis. Soldering and Surface Mount Technology. 2001;13(1):27-34.
17. Xiao Q, Nguyen L, Armstrong WD. Aging and creep behavior of Sn3.9Ag0.6Cu solder alloy. In: Proceedings of the 54th Electronic Components and Technology Conference; 2004. p. 1325-1332.
18. Smetana J, Horsley R, Lau JH, *et al*. iNEMI lead-free strategic roadmap version 4.0. In: Proceedings of SMTA International; 2021. p. 245-258.
19. Zhang Y, Cai Z, Suhling JC, Lall P, Bozack MJ. The effects of aging temperature on SAC solder joint material behavior and reliability. In: Proceedings of the 58th Electronic Components and Technology Conference; 2008. p. 99-112.